Determining Lithium Abundance from Classical Nova Ejecta

Jerry Yeung[1] and Frederick Walter[1]

[1]*Department of Physics and Astronomy, Stony Brook University, Stony Brook, NY 11794-3800, USA*

ABSTRACT

1. INTRODUCTION

Big Bang Nucleosynthesis (BBN) produced the universe's first lithium within roughly 3 minutes after the Big Bang(see Figure 1.). According to the models (Cyburt et al. 2015), this same process also produce light nuclei such as deuterium, helium, and a trace amount of lithium. In the standard model of cosmology (SBBN), the primordial abundances of these elements depend primarily on the baryon-to-photon ratio(Izzo et al. 2015). Recent measurements of the cosmic microwave background from Wilkinson Microwave Anisotropy Probe (WMAP) and Planck satellite have obtained the ratio with a very high accuracy with a predicted primordial lithium abundance of $(^7\text{Li/H})_{\text{BBN+CMB}} = (4.94\pm0.72)\times 10^{-10}$ (Yeh et al. 2021; Fields & Olive 2022) or on a log scale A(Li) $\sim$ 2.72 (Planck Collaboration et al. 2016). This value is different from the observed abundance of $(^7\text{Li/H})_{\text{obs}} = (1.6 \pm 0.3) \times 10^{-10}$ (Fields & Olive 2022) or A(Li) $\sim$ 2.2 in the atmospheres of old, metal-poor stars on the Spite plateau, a discrepancy known as the cosmological lithium problem(Spite & Spite 1982).

One explanation is that the observed discrepancy results from the post-formation depletion of primordial lithium in stellar interiors (Miranda 2025). This occurs because ^7Li fuses at the relatively low temperature of 2.5 million Kelvin. In the old, cooler stars used to measure primordial abundances, the outer convective zone is deep, acting more like a conveyor belt that transports surface material down into hot interior regions where lithium is destroyed. Stellar models incorporating atomic diffusion and these transport mechanisms can account for a significant portion of this reduction in old stars (Miranda 2025).

A different explanation involves non-standard physics to alter the primordial nucleosynthesis process. The existence of previously unknown particles or modifications to fundamental interactions could have intervened to reduce the final lithium yield predicted by BBN (Fields 2011), see Miranda (2025) for a detailed review.
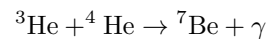
While these two explanations seek to explain the primordial lithium deficit, a separate astrophysical question is the origin of later lithium enrichment. The lithium seen in very old, metal-poor stars reflects that primordial level and only acts as a baseline for galactic chemical evolution. Younger stars(Lyubimkov 2016), as well as the composition of our Solar System traced by meteorites(Matteucci et al. 2021), show roughly 10-12 times more lithium than that value, which implies that other astrophysical processes must have produced additional lithium.

Several production sites have been proposed to explain this excess. Asymptotic Giant Branch (AGB) stars may contribute to Galactic lithium enrichment through the Cameron–Fowler mechanism operating during HBB (Ventura & D'Antona 2009). Cosmic-ray spallation also produces lithium when high-energy protons and α-particles collide with interstellar C, N, and O nuclei (Meneguzzi et al. 1971). Classical novae are now considered a major contributor since the explosive hydrogen burning on the surface of accreting white dwarfs can efficiently synthesize ^7Be, which later decays to ^7Li (Tajitsu et al. 2015; Izzo et al. 2015; Cescutti & Molaro 2018).

1.1. *Asymptotic giant branch (AGB) stars*

AGB stars can produce lithium through processes such as proton ingestion events (PIEs) and Hot bottom burning(HBB), both relying on the Cameron-Fowler mechanism, which is the process by which stars produce ^7Li(Cameron & Fowler 1971). At high temperatures (typically T $> 10^7$ K), ^3He and ^4He nuclei fuse via the reaction

$$^3\text{He} +^4 \text{He} \rightarrow {}^7\text{Be} + \gamma$$

The resulting ^7Be is radioactive and must be transported to cooler outer layers ($T < 10^6$ K) via large-scale convection before it is destroyed by proton captures (Ventura & D'Antona 2009). Once in the cooler envelope, the ^7Be nuclei undergo electron capture, decaying into stable ^7Li (see Eqn 1) with the emission of a 0.86 MeV neutrino (Izzo et al. 2015). In high-mass AGB stars ($>$3–4 $M_\odot$), HBB occurs when the base of the deep convective envelope is hot enough to activate the proton-capture reactions of the Cameron-Fowler mechanism, while in low-mass AGB stars (1–3 $M_\odot$), PIEs are triggered when a convective zone from a thermal pulse extends into the
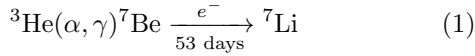
hydrogen-rich envelope. Protons are transported downward into hot burning regions (Choplin et al. 2022), where the rapid nuclear reactions produce ^{7}Be, and leads to lithium enrichment with surface abundances reaching A(Li) $\approx$ 3 to 5. However, recent observational studies indicate that AGB stars alone cannot account for the meteoritic lithium abundances, suggesting that other sources are required to explain the observed galactic lithium problem (Borisov et al. 2024).

1.2. *Galactic cosmic-ray spallation*

Lithium is synthesized in the interstellar medium when high-energy protons and cosmic rays collide with C, N, O. These collisions cause the target nuclei to expel nucleons and form light elements like lithium, beryllium(Vangioni-Flam et al. 1998; Laumer et al. 1973). This is a primary non-thermal nucleosynthesis pathway for lithium, especially for the isotope ^{6}Li. In a survey for the Small Magellanic Cloud, 'Ciprijanovi'c (2016) stated that galactic cosmic rays could only produce a very small amount of lithium in the Small Magellanic Cloud, with only 0.16% of the measured abundance explained by this source.

1.3. *Classical Novae*

During a classical nova explosion, extreme temperatures ($\sim$100 to 200 million K during the explosion) enable the nuclear reaction ^{3}He$(\alpha, \gamma)^7$Be, producing radioactive ^{7}Be. This ^{7}Be is then transported outward in the nova ejecta, and in order to decay into ^{7}Li, ^{7}Be must avoid destruction from further proton captures in the hot remnant before the ejecta thins. As the ejected shell expands and cools over time, the ^{7}Be decays with a half-life of $\sim$53 days, transforming into ^{7}Li via

$$^3\text{He}(\alpha, \gamma)^7\text{Be} \xrightarrow[\text{53 days}]{e^-} {^7}\text{Li} \qquad (1)$$

This process, proposed by Starrfield et al. (1978), is now recognized as a primary pathway for ^{7}Li production in nova explosions. The evidence includes the detection of blue-shifted ^{7}Be II lines in the ultraviolet spectra of several classical novae, such as V339 Del (Tajitsu et al. 2015), V5668 Sgr (Molaro et al. 2016), and V2944 Oph (Tajitsu et al. 2015). The blueshifts confirms the ^{7}Be is indeed in the rapidly outflowing ejecta and not the surrounding medium. However, Shore, Steven N. & De Gennaro Aquino, Ivan (2020) presented NLTE spectral models demonstrating that the $\lambda \sim 3131$ Å feature attributed to ^{7}Be II in novae like V838 Her can be reproduced by a blend of other species in models with only solar composition, without requiring a beryllium overabundance. Their models also showed that for the reported extreme overabundances, the ^{7}Be II line should

be far stronger than what is observed, doubting on these initial identifications and the derived abundances.

Izzo et al. (2015) reported a direct detection of ^{7}Li in the early optical spectra of Nova V1369 Cen (see Figure 2). The measured ^{7}Li abundance in the nova ejecta is significantly higher than solar values, the Li/Na ratio to the solar system abundance of sodium, A(Na) $\sim$ 6.30(Lodders et al. 2009), yields a ^{7}Li abundance of A(Li) $\sim$ 4.8 using A(Li)/A(Na) = 2.4/100(Izzo et al. 2015), suggesting classical novae are sufficient to explain the observed overabundance of lithium in young stellar populations. Note that V1369 Cen was a 'slow' nova, means it has a slow light curve evolution with a decline time. The slower expansion of the ejecta in classical novae is important because it gives ^{7}Be sufficient time to decay into ^{7}Li before the ejecta becomes too diffuse to observe(Tajitsu et al. 2015; Molaro et al. 2016). The slower radial velocity also results in narrower spectral lines, making the detection of the lithium line easier(Selvelli et al. 2018). In contrast, a 'fast' nova, the thin ejecta and very broad spectral lines would make the specific identification of the lithium line far more challenging.
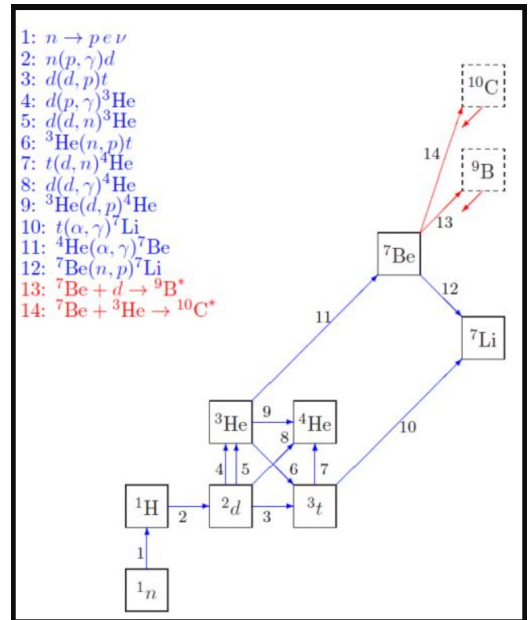

Figure 1. Simplified nucleosynthesis network from Fields (2011), showing pathways for lithium production in both primordial and galactic evolution. The network shows how deuterium starts the reaction chains leading to ^{3}He, ^{4}He, and ultimately to ^{7}Li and ^{7}Be.

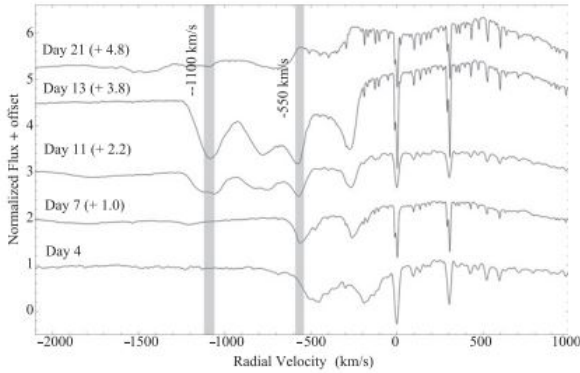**Figure 2.** Figure from Izzo et al. (2015), showing identified blueshifted ^{7}Li I 6708 Å, moving at –550 km/s. Note that the absorption feature is only prominent between days 7 to 13.

2. METHOD

The detection of lithium in nova ejecta relies on identifying the resonance doublet of ^{7}Li I at $\lambda \sim 6707.81$ Å. This is challenging due to the line's intrinsic weakness, potential blending with other species like Fe I 6707.44 Å, and in fast novae, line broadening from high-velocity ejecta that reduces the peak depth of the feature, which would make it harder to detect against the continuum. The detection of ^{7}Li in novae, as demonstrated by Izzo et al. (2015), Tajitsu et al. (2015), and Molaro et al. (2016), requires high-resolution spectroscopy timed to catch either the short-lived ^{7}Be or its decay product, ^{7}Li. Tajitsu et al. (2015) demonstrated that the most direct approach is to observe ^{7}Be before it decays using high-resolution ($R \sim 90,000$–$60,000$) ultraviolet spectroscopy, targeting the ^{7}Be II resonance doublet at $\lambda \sim 3130.58$ Å, $\lambda \sim 3131.07$ Å within 50 days of outburst. This requires high spectral resolution to resolve the doublet and measure its blueshift to confirm its origin in the ejecta. Izzo et al. (2015) used high-resolution ($R \sim 48,000$) optical spectra to monitor the ^{7}Li I 6708 Å line starting immediately after outburst. They found the blueshifted lithium line appears when the ejecta are sufficiently cool for neutral lithium to form but before the line dilution, which would make it undetectable. Both use spectral modeling to confirm line identifications and calculate abundances from equivalent widths.

We will apply these methods to search for the ^{7}Li I 6707.81 Å line in 33 different novae. For each object, we inspected all available spectra covering the 6680–6720 Å region, with particular focus on around 60 days post-outburst when approximately half-lives of ^{7}Be had passed(see Eqn. 1), and any ^{7}Be detected at early times should have substantially decayed to ^{7}Li. We searched for absorption features at blueshifted and red-

shifted velocities consistent with other ejecta lines (e.g., Na I 5889.951 Å , Ca I 6717 Å, Fe II 5018 Å, and Ca I 4227 Å) in the same spectrum. We used the Na I D line at 5889.951 Å because neutral sodium and neutral lithium have similar first ionization potentials (5.14 eV and 5.39 eV, respectively), meaning they co-exist in similar regions and temperatures within the ejecta. Furthermore, we used the Ca I 4227 Å line, following the methodology of Molaro et al. (2016), who demonstrated its value as a reliable tracer for the kinematic structure of the neutral gas component in which lithium forms.

3. OBSERVATION OF ^{7}LI I 6707.81 Å

Spectra of 33 classical novae from the Stony Brook/SMARTS Spectral Atlas of Southern Novae (6680–6720 Å) were analyzed to detect and measure the equivalent width of the ^{7}Li line. The data reduction pipeline included cosmic-ray rejection that preserves emission lines, boxcar extraction with interorder background subtraction, proper error propagation, and optional Gaussian extraction. To extend the wavelength coverage, orders 126–138 (4085–4510 Å), which are not extracted in standard reductions, were fully processed—extracting all 1028 pixels per order (compared to the standard 800), which enabling complete spectral coverage to 8300 Å without the interorder gaps that typically appear beyond 6500 Å. Final flux calibration and order splicing produced one-dimensional spectra spanning 4085–8900 Å. Among the 33 novae examined, only five novae exhibited prominent Li I 6707.81 Å absorption features suitable for equivalent width measurements, V1369 Cen, V906 Car, V6594 Sgr, V5668 Sgr, and V5667 Sgr.

We used Gaussian profile fitting to measure equivalent widths of the lithium feature. For each nova, we performed single or multi-component Gaussian fits to account for possible line blending or multiple velocity components in the ejecta. The continuum was normalized using selected continuum points on either side of the absorption line to ensure accurate equivalent width measurements.

We then can turn the centroid(λ_{obs}) into radial velocity via doppler shift formula

$$v_r = c \cdot \frac{\lambda_{\text{obs}} - \lambda_{\text{rest}}}{\lambda_{\text{rest}}} \qquad (2)$$

where v_r is the radial velocity, c is the speed of light, λ_{obs} is the observed centroid wavelength, and λ_{rest} is the rest wavelength. Typical uncertainties in v_r are on the order of 10–20 km s^{-1}, mainly from wavelength calibration and line-profile asymmetry. Equivalent-width
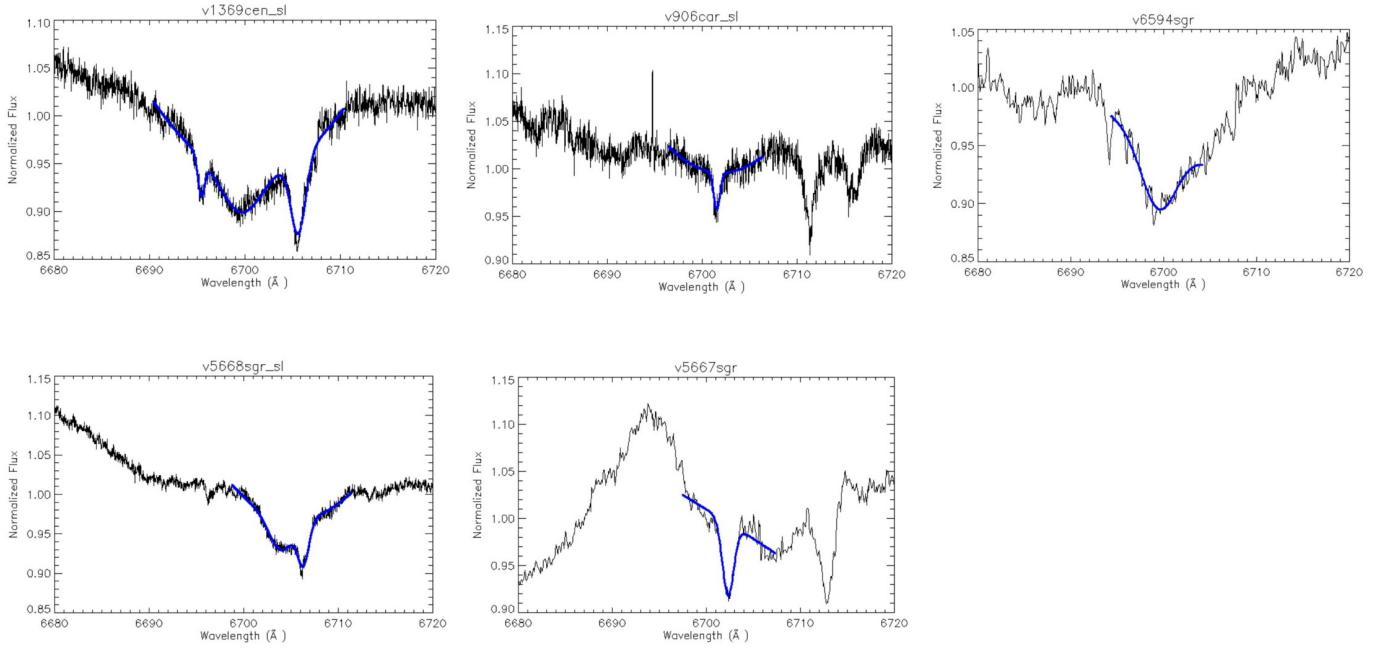
Figure 3. Normalized spectra of five classical novae showing the region 6680–6720 Å. Gaussian fits to the lithium absorption feature are overplotted in blue. All spectra show clear absorption around 6702 Å. Note the depth and profile of the absorption vary among the novae, result from differences in lithium abundance.

uncertainties were derived from the IDL Gaussian-fitting function, which estimates parameter errors based on the covariance matrix of the fit.

To verify the ^{7}Li I detection, we required that the radial velocity be consistent (within 3σ) with that of other neutral lines, such as Na I 5889.951 Å , Ca I 6717 Å, Fe II 5018 Å, and Ca I 4227 Å, in the same spectrum. This ensured that the absorption originated from the nova ejecta rather than other interstellar objects. We also verified that the feature does not coincide with known telluric absorption bands.

The equivalent widths W_λ were computed directly from the best-fitting Gaussian models. The resulting W_λ values and their uncertainties were then converted into column densities N using the formula from Gray (2005) under the assumption of optically thin absorption

$$W_\lambda = \frac{\pi e^2}{m_e c^2} N f \lambda^2 \qquad (3)$$

Converting from cgs units to the practical units used in observation (W_λ and λ in Å), and substituting the numerical values of the physical constants, we get

$$N = 1.13 \times 10^{20} \frac{W_\lambda}{\lambda^2 f} \qquad (4)$$

where λ is the rest wavelength in Å, W_λ is the equivalent width in Å, and f is the oscillator strength of the Li I 6707.81 Å transition ~ 0.75 (Morton 2003). This provides a first-order estimate of the lithium column den-

sity in the line-forming region. The assumption of optical thinness is justified by the relatively weak equivalent widths ($W_\lambda \leq 1$ Å) observed in all five novae.

4. MODEL

Assuming Local Thermodynamic Equilibrium (LTE), we model the evolution of the lithium absorption equivalent width. Consider the nova ejecta as an expanding spherical shell, at time t after outburst, the shell has expanded to radius $R(t) = v_{\exp} \cdot t$ where $v_{\exp}$ is the observed expansion velocity of the ejecta obtained using Equation 2. This shell lies between the observer and the background white dwarf photosphere. The fraction of the WD photosphere obscured by the absorbing shell determines the strength of the absorption line. For a white dwarf of radius $R_{\rm WD}$, the solid angle of the white dwarf as seen from Earth is proportional to its cross-sectional area, $\pi R_{\rm WD}^2$. The absorbing shell, at distance $R(t)$ from the center, covers a ring on the sky whose width depends on the shell thickness ΔR (assumed $v_{\exp}$ constant). The covering fraction $f_{\rm cov}(t)$ is fraction of the WD disk blocked by lithium, for $R(t) \gg R_{WD}$ it scales approximately as

$$f_{\rm cov}(t) \approx \frac{\text{Area of shell overlapping WD}}{\text{Area of WD}} \propto \left(\frac{R_{\rm WD}}{R(t)} \right)$$

Consider initial conditions, at early times, when $R(t)$ is only slightly larger than $R_{\rm WD}$, nearly the entire WD is covered, yielding maximum absorption depth. As the

shell expands, $R(t)$ increases and the covering fraction decreases.

In the optically thin limit, the equivalent width W_λ of the absorption line is proportional to both the covering fraction and the column density of absorbing atoms $N_{\rm Li}$ (Gray 2005)

$$W_\lambda(t) \propto f_{\rm cov}(t) \cdot N_{\rm Li}$$

If the total number of lithium atoms in the shell is conserved (no nuclear destruction or creation after the early explosive nucleosynthesis), then the column density scales inversely with the shell's surface area (van Marle, A. J. & Keppens, R. 2012)

$$N_{\rm Li} \propto \frac{1}{R(t)^2}$$

So we get

$$W_\lambda(t) \propto f_{\rm cov}(t) \cdot \frac{1}{R(t)^2} \propto \left(\frac{R_{\rm WD}}{R(t)}\right) \cdot \frac{1}{R(t)^2} = \left(\frac{R_{\rm WD}}{v_{\rm exp}^2}\right)^2 \frac{1}{t^2}$$

This t^{-2} decline reflects the dilution of the absorbing material over a larger surface area as the shell expands. The geometrical dilution alone would predict a steady decline in equivalent width, but the ejecta also cools, altering the ionization and excitation balance of lithium. Newton's law of cooling is considered for the ejecta temperature $T_e(t)$

$$\frac{dT_e}{dt} = -k\left[T_e(t) - T_{\rm env}\right]$$

$$T_e(t) = T_{\rm env} + (T_0 - T_{\rm env})e^{-kt}$$

where $T_{\rm env}$ is the temperature of the surrounding, and k is a cooling rate constant. If $T_{\rm env} = 0$, then it is a simplified exponential cooling law for the ejecta temperature $T_e(t)$

$$T_e(t) = T_0 e^{-t/\tau_{\rm cool}}$$

Here $T_0 = 10,000 \sim 11,000\,{\rm K}$ is the initial outburst temperature and $\tau_{\rm cool} = 1/k$ is the cooling timescale.

The ionization balance between Li I and Li II is given by the Saha equation

$$\frac{n_{\rm Li\,II}}{n_{\rm Li\,I}} = \frac{1}{n_e}\left(\frac{2\pi m_e k_B T_e}{h^2}\right)^{3/2}\frac{2U_{\rm Li\,II}(T_e)}{U_{\rm Li\,I}(T_e)}\exp\left(-\frac{\chi_{\rm Li\,I}}{k_B T_e}\right)$$

where n_e is the electron density (decreasing as t^{-3} due to expansion), $\chi_{\rm Li\,I} = 5.39\,{\rm eV}$ is the ionization potential of neutral lithium, $U_{\rm Li\,I}$, $U_{\rm Li\,II}$ are partition functions. The fraction of lithium in the neutral state (Li I) is

$$f_{\rm Li\,I}(t) = \frac{n_{\rm Li\,I}}{n_{\rm Li}} = \left[1 + \frac{n_{\rm Li\,II}}{n_{\rm Li\,I}}\right]^{-1}$$

As the ejecta cools, $f_{\rm Li\,I}$ increases because the exponential term $\exp(-\chi_{\rm Li\,I}/k_B T_e)$ grows rapidly when $k_B T_e \ll \chi_{\rm Li\,I}$.

The 6707.81 Å absorption line arises from the Li I ground state. The fraction of neutral lithium in the ground state, $f_{\rm gs}$, is given by the Boltzmann distribution

$$f_{\rm gs}(t) = \frac{g_0}{U_{\rm Li\,I}(T_e)}\exp\left(-\frac{E_0}{k_B T_e}\right)$$

where $g_0 = 2$ is the statistical weight of the ground state and $E_0 = 0$. For low excitation temperatures and relatively low densities, most neutral lithium resides in the ground state, so $f_{\rm gs} \approx 1$ once $T_e \lesssim 8000\,{\rm K}$.

The equivalent width of the Li I 6707.81 Å line can now be expressed as

$$W_\lambda(t) \propto f_{\rm cov}(t) \cdot N_{\rm Li} \cdot f_{\rm Li\,I}(t) \cdot f_{\rm gs}(t)$$

Substituting the time dependencies

$$W_\lambda(t) \propto \frac{1}{t^2} \cdot f_{\rm Li\,I}\big(T_e(t)\big) \cdot f_{\rm gs}\big(T_e(t)\big)$$

The ionization term $f_{\rm Li\,I}(t)$ increases with time as the ejecta cools, partially offsetting the geometric t^{-2} decline.

REFERENCES

Borisov, S., Prantzos, N., & Charbonnel, C. 2024, A&A,
  doi: 10.1051/0004-6361/202451321

Cameron, A. G. W., & Fowler, W. A. 1971, ApJ, 164, 111,
  doi: 10.1086/150821

Cescutti, G., & Molaro, P. 2018, MNRAS,
  doi: 10.1093/mnras/sty2967

Choplin, A., Siess, L., & Goriely, S. 2022, A&A,
  doi: 10.1051/0004-6361/202244360

'Ciprijanovi'c, A. 2016, Astropart. Phys., 85,
  doi: 10.1016/j.astropartphys.2016.09.004

Cyburt, R., Fields, B., Olive, K., & Yeh, T.-H. 2015, RMP,
  88, doi: 10.1103/RevModPhys.88.015004

Fields, B. 2011, Annu. Rev. Nucl. Part. Sci., 61,
  doi: 10.1146/annurev-nucl-102010-130445

Fields, B. D., & Olive, K. A. 2022, Implications of the
  Non-Observation of ^{6}Li in Halo Stars for the Primordial
  ^{7}Li Problem. https://arxiv.org/abs/2204.03167

Gray, D. F. 2005, The Observation and Analysis of Stellar Photospheres, doi: 10.1017/CBO9781316036570

Izzo, L., Valle, M., Mason, E., et al. 2015, ApJL, 808, doi: 10.1088/2041-8205/808/1/L14

Laumer, H., Austin, S., Panggabean, L. M., & Davids, C. 1973, PRC, 8, doi: 10.1103/PHYSREVC.8.483

Lodders, K., Palme, H., & Gail, H.-P. 2009, LB, 4B, 712, doi: 10.1007/978-3-540-88055-4_34

Lyubimkov, L. S. 2016, Astrophysics, 59, 411, doi: 10.1007/s10511-016-9446-5

Matteucci, F., Molero, M., Aguado, D., & Romano, D. 2021, doi: 10.1093/mnras/stab1234

Meneguzzi, M., Audouze, J., & Reeves, H. 1971, A&A, 15, 337

Miranda, O. D. 2025, A&A, 701, A164, doi: 10.1051/0004-6361/202554482

Molaro, P., Izzo, L., Mason, E., Bonifacio, P., & Valle, M. 2016, MNRAS, 463, doi: 10.1093/mnrasl/slw169

Morton, D. C. 2003, ApJ, 149, 205, doi: 10.1086/377639

Planck Collaboration, Ade, P. A. R., Aghanim, N., et al. 2016, A&A, 594, A13, doi: 10.1051/0004-6361/201525830

Selvelli, P., Molaro, P., & Izzo, L. 2018, MNRAS, doi: 10.1093/mnras/sty2310

Shore, Steven N., & De Gennaro Aquino, Ivan. 2020, A&A, 639, L12, doi: 10.1051/0004-6361/202038599

Spite, F., & Spite, M. 1982, A&A, 115, 357

Starrfield, S., Truran, J., & Sparks, W. 1978, ApJ, 226, doi: 10.1086/156598

Tajitsu, A., Sadakane, K., Naito, H., Arai, A., & Aoki, W. 2015, Nature, 518, doi: 10.1038/nature14161

van Marle, A. J., & Keppens, R. 2012, AA, 547, A3, doi: 10.1051/0004-6361/201218957

Vangioni-Flam, E., Cassé, M., Cayrel, R., et al. 1998, New Astron., 4, doi: 10.1016/S1384-1076(99)00015-9

Ventura, P., & D'Antona, F. 2009, MNRAS, 402, doi: 10.1111/j.1745-3933.2010.00805.x

Yeh, T.-H., Olive, K. A., & Fields, B. D. 2021, JCAP, 2021, 046, doi: 10.1088/1475-7516/2021/03/046